Characterization of an Unfolding Intermediate and Kinetic Analysis of Guanidine Hydrochloride-Induced Denaturation of the Colicin E1 Channel Peptide†

Brian A. Steer‡ and A. Rod Merrill*

Guelph-Waterloo Centre for Graduate Work in Chemistry, Department of Chemistry and Biochemistry, University of Guelph, Guelph, Ontario, Canada N1G 2W1

Received August 2, 1996; Revised Manuscript Received November 14, 1996⊗

ABSTRACT: The equilibrium unfolding pathway of the colicin E1 channel peptide was shown in a previous study to involve an unfolding intermediate, stable in approximately 4 M guanidine hydrochloride, which comprised primarily the C-terminal hydrophobic α-helical hairpin segment of the peptide [Steer, B. A., & Merrill, A. R. (1995) *Biochemistry 34,* 7225−7233]. In this study, the structural nature of this unfolding intermediate was investigated further, and it was found that the intermediate primarily consists of a dimer species and is comprised of two partially denatured monomeric peptides, which appear to be associated by hydrophobic interactions. The dimerized structure was detected by size-exclusion high-performance liquid chromatography, sodium dodecyl sulfate−polyacrylamide gel electrophoresis, chemical cross-linking, and intermolecular fluorescence energy transfer. Using stopped-flow fluorescence spectroscopy, the kinetics of the denaturation and dimerization of the colicin E1 channel peptide in 4 M guanidine hydrochloride were examined. Denaturation kinetics were also investigated by wild-type peptide Trp fluorescence and 1-anilinonaphthalene-8-sulfonic acid binding. The kinetics of dimer formation were examined by monitoring the time dependence of intermolecular Trp to 5-[[2-[(iodoacetyl)amino]ethyl]amino]naphthalene-1-sulfonic acid fluorescence resonance energy transfer upon denaturation in 4 M guanidine hydrochloride. In addition, single Trp mutant peptides were employed as site-specific fluorescent probes of unfolding kinetics and reported diverse and characteristic unfolding kinetics. However, it was shown that following a rapid and major unfolding transition the peptide's core residues cluster slowly, by hydrophobic association, forming an intermediate species which is a prerequisite to dimerization. These equilibrium and kinetic unfolding data describe a unique unfolding mechanism where the channel peptide forms a partially unfolded dimerized structure in 4 M guanidine hydrochloride.

The toxin-like colicin E1 protein is a channel-forming bacteriocin secreted by *Escherichia coli* which carry the naturally occurring *colE1* plasmid. It exerts its toxic effects by forming a lethal ion channel in the target bacterium which depolarizes the membrane sufficiently to cause cell death (Gould & Cramer, 1977; Cleveland *et al.,* 1983; Bullock, 1992; Cramer *et al.,* 1995). The 522 amino acid colicin E1 primary structure can be divided into 3 functional domains. The receptor binding domain of colicin E1 binds to the vitamin B_{12} receptor in the outer membrane of the target bacterium. The N-terminal translocation domain is involved in translocating the protein across the outer membrane, and the C-terminal channel-forming domain forms a dissipative ion channel in the cytoplasmic membrane. The channel-forming domain of colicin E1 is compact and protease resistant and can be conveniently isolated from the translocation and receptor binding domains of colicin E1 by treatment of whole colicin E1 with protease (Cramer *et al.,* 1990, 1995). Lacking its receptor binding and translocation domains, the channel-forming peptide (channel peptide) cannot penetrate the outer membrane of target bacterial cells. However, the channel peptide forms active channels in osmotically shocked whole cells (Cramer *et al.,* 1983) and, upon low pH-induced *in vitro* activation, forms ion-conducting pores in membrane vesicles (Peterson & Cramer, 1987; Schendel & Cramer, 1994) and in planar bilayers (Bullock *et al.,* 1983).

The preliminary crystal structure of the soluble colicin E1 channel peptide has been elucidated (Elkins *et al.,* 1995). The highly α-helical colicin E1 channel peptide has 10 helical segments arranged in 3 layers with 2 distinctively hydrophobic antiparallel helices (helices 8 and 9) buried within the core of the structure. Amphipathic surface helices surround the peptide's particularly hydrophobic core, shielding it from aqueous solvent giving rise to a soluble peptide.

Unfolding of the colicin E1 channel peptide in guanidine hydrochloride (Gn-HCl)[1] has been shown to involve a partially denatured equilibrium unfolding intermediate which

† This work was supported by a grant from the Natural Sciences and Engineering Research Council of Canada (A.R.M.) and by a predoctoral scholarship from the Natural Sciences and Engineering Research Council of Canada (B.A.S).

* Author to whom correspondence should be addressed (telephone, 519-824-4120, ext. 3806; fax, 519-766-1499; e-mail, merrill@chembio.uoguelph.ca).

‡ Present address: Department of Biology, 68-230, Massachusetts Institute of Technology, 77 Massachusetts Ave., Cambridge, MA 02139.

⊗ Abstract published in *Advance ACS Abstracts,* February 15, 1997.

[1] Abbreviations: AEDANS, 5-[[2-[(acetyl)amino]ethyl]amino]-naphthalene-1-sulfonic acid; ANS, 1-anilinonaphthalene-8-sulfonic acid; C-terminal, carboxy-terminal; DMG, dimethylglutaric acid; FRET, fluorescence resonance energy transfer; Gn-HCl, guanidine hydrochloride; HPLC, high-performance liquid chromatography; IAEDANS, 5-[[2-[(iodoacetyl)amino]ethyl]amino]-naphthalene-1-sulfonic acid; k_{app}, apparent rate constant; k_f, fast unfolding rate constant; k_s, slow unfolding rate constant; M_r, relative mobility; M_w, molecular weight; R_S, Stokes' radius; SDS−PAGE, sodium dodecyl sulfate−polyacrylamide gel electrophoresis; $t_{1/2}$, unfolding reaction half-life; Trp^-, colicin E1 mutant channel peptide devoid of Trp residues; V_e, elution volume; WT, wild-type.

S0006-2960(96)01926-5 CCC: $14.00

is stable in approximately 4 M guanidine hydrochloride (Gn-HCl; Steer & Merrill, 1995). Site-specific examination of the peptide's unfolding using the fluorescence of single Trp mutant peptides demonstrated that the intermediate primarily involved the peptide's hydrophobic α-helical hairpin core segment. The intermediate was also shown to bind the hydrophobic fluorescent probe 1-anilinonaphthalene-8-sulfonic acid (ANS) maximally over the native and unfolded states and to possess little secondary structure as determined by circular dichroism spectroscopy. These data described a partially denatured intermediate species consisting of a cluster of hydrophobic core residues with little secondary structure (Steer &Merrill, 1995, 1996).

This study further characterizes the structural nature of this equilibrium unfolding intermediate and describes a hydrophobically associated dimerized intermediate structure. Since the peptide's dimerization appears to involve hydrophobic core association of partially denatured monomeric peptides, dimerization may occur after a major unfolding transition which would expose the peptide's nonpolar core residues. Thus, the kinetics of the peptide's denaturation to this intermediate structure and its dimerization in 4 M Gn-HCl were examined.

Stopped-flow spectroscopic techniques allow the monitoring of fast unfolding events on the millisecond time scale. Kinetic analysis can often detect the presence of unfolding intermediates and structural rearrangements not observed in equilibrium studies. Through the use of single Trp mutant proteins and stopped-flow fluorescence spectroscopy, the kinetics of denaturation of specific peptide segments can be investigated. The kinetic data presented in this study describe a possible kinetic route for the peptide's unfolding and dimerization in 4 M Gn-HCl.

MATERIALS AND METHODS

Preparation of Mutants and Isolation of Colicin E1 and Its Thermolytic Channel Peptide. Single Trp mutants of colicin E1 were constructed by site-directed mutagenesis as already described (Merrill *et al.*, 1993). Colicin E1 was purified from a lex A^- *E. coli* strain (IT3661, kindly provided by Irwin Tessman) harboring the plasmid $pSKE1^-$ which encoded the appropriate mutant as detailed previously (Merrill *et al.*, 1993). Trp^- peptide−AEDANS adduct was prepared exactly as described earlier (Steer & Merrill, 1994).

Size-Exclusion Chromatography. Size-exclusion chromatography was performed using a Superose 6 column (1.25 cm in diameter by 40 cm in length) attached to a Bio-Rad (Mississauga, ON) Model 2700 HPLC solvent delivery system equipped with a Model 1706 UV/VIS detector. For Stokes' radius (R_S) estimation, the column was calibrated according to Beattie and Merrill (1996) using the standard proteins, ribonuclease A (R_S, 16.4 Å), chymotrypsinogen (R_S, 20.9 Å), ovalbumin (R_S, 30.5 Å), albumin (R_S, 35.5 Å), alcohol dehydrogenase (R_S, 45.5 Å), apoferritin (R_S, 61.0 Å), and thyroglobulin (R_S, 85.0 Å). In order to examine the effects of Gn-HCl on the channel peptide's R_S, the colicin E1 C-terminal thermolytic channel peptide, in 100 mM NaCl/10 mM dimethylglutaric acid (DMG) buffer, pH 6.0, was mixed with the appropriate amount of 8 M sequenal grade Gn-HCl purchased from Pierce (Rockford, IL) to provide solutions from 0 to 7 M Gn-HCl and 0.25 mg/mL channel peptide, final concentration. The column was equilibrated with the appropriate concentration of denaturant prior to injection of the sample. Sample elution was detected by the absorbance at 280 nm.

SDS−PAGE and Chemical Cross-Linking. The denatured peptide was also subject to SDS−PAGE. The peptide (0.5 mg/mL) was denatured in various concentrations of Gn-HCl and incubated as described above. Following incubation, the peptide samples were diluted 10-fold with 100 mM NaCl in 10 mM DMG buffer, pH 6.0 (a high concentration of Gn-HCl interferes with the electrophoresis process), and SDS−PAGE was immediately performed (samples were loaded and running in less than 5 min after dilution) according to Laemmli (1970). For cross-linking experiments, the peptide (tested in a range from 1 to 6 mg/mL, final concentration) was denatured in various concentrations of Gn-HCl containing 50 mM MES buffer at pH 6, 100 mM NaCl, and 10 mM of the water-soluble carbodiimide 1-ethyl-3-[3-(dimethylamino)propyl]carbodiimide hydrochloride (EDC) as suggested by Buisson and Reboud (1982), and the reaction was allowed to proceed for 1 h at 20 °C. The reaction was quenched by the addition of sodium acetate and NH_4Cl at 20 and 100 mM, respectively. The samples were then diluted 5-fold with distilled water prior to SDS−PAGE analysis.

Steady-State Spectroscopic Measurements. Fluorescence emission spectra were recorded on a PTI Alphascan-2 spectrofluorometer (PTI, South Brunswick, NJ) equipped with a jacketed cell holder set at 20 °C. For all fluorescence measurements, a wedge depolarizer (Oriel Corp., Stratford, CT; 95% transmittance) was placed on the exit side of the excitation monochromator, and fluorescence emission was detected at right angles. Steady-state Trp fluorescence emission was scanned from 303 to 450 nm (4 nm slit) upon 295 nm excitation (2 nm slit). Corrections were made for the appropriate blanks and for the wavelength-dependent bias of the optical and detection systems. In Trp−AEDANS fluorescence resonance energy transfer (FRET) experiments, the sample was excited at 295 nm and the emission scanned from 303 to 575 nm with a 3 nm excitation band-pass and a 6 nm emission band-pass. Intermolecular Trp−AEDANS FRET was measured with Trp^- peptide−AEDANS adduct at a fixed concentration of 0.1 mg/mL and denatured in 4 M Gn-HCl. The denatured adduct was titrated with wild-type (WT) peptide in 0.015 mg/mL increments.

Model for Peptide Association upon Denaturation. The degree of association of colicin E1 channel peptides upon denaturation in 4 M GnHCl was investigated using FRET from a donor population (three Trp residues in the WT peptide) to an acceptor population (AEDANS−Trp^- channel peptide, no Trp donor). Derived from Forster theory, the model is as follows: Supposing that the colicin E1 channel is dimeric, let [DD] = the concentration of pure WT (donor) channel peptide dimers; let [AA] = the concentration of pure AEDANS−Trp^- (acceptor) channel peptide dimers; and let [AD] = the concentration of hybrid channel peptide dimers. The efficiency of energy transfer between a donor and acceptor pair, E, is defined by eq 1 (Lakowicz, 1983) in which Q/Q_o is the relative quantum yield of the donor species.

$$E = 1 + Q/Q_o \quad (1)$$

For energy transfer occurring within a hybrid dimer (where the acceptor fluorescence is measured), the total dimer

quantum yield, Q_o, is given by

$$Q_o = 2[AA] + [AD] \quad (2)$$

This relationship accounts for all acceptor molecules within the system. The quantum yield of the acceptor species in the presence of the donor species, Q, is given by eq 3:

$$Q = 1 + E[AD] + 2[AA] \quad (3)$$

Here, the acceptor quantum yield of the heterodimer (AD) is proportional to the efficiency of energy transfer. Taking the ratio of eqs 2 and 3, the relative acceptor quantum yield is obtained (eq 4).

$$Q/Q_o = 1 + E[AD]/(2[AA] + [AD]) \quad (4)$$

To convert the concentrations in eq 4 to a measurable quantity, the probabilities of forming each type of dimer must be considered. Let P_A, P_D, and P_H represent the probabilities of forming pure acceptor dimer, pure donor dimer, and pure hybrid dimer, respectively. Then,

$$P_A = a^2 = \{[A]/([A] + [D])\}^2 \quad (5)$$

$$P_D = d^2 = \{[D]/([A] + [D])\}^2 \quad (6)$$

$$P_H = 2ad = 2\{[A][D]/([A] + [D])^2\} \quad (7)$$

where a is the acceptor mole fraction and d is the donor mole fraction. Substituting the following relationship is obtained:

$$Q/Q_o = 1 + E(2ad)/(2[A]^2 + 2ad) \quad (8)$$

$$Q/Q_o = 1 + dE/(a + d) \quad (9)$$

since $a + d = 1$ then

$$Q/Q_o = 1 + dE \quad (10)$$

The more general form of eq 10 is

$$Q/Q_o = 1 + E - E(1 - d)^{n-1} \quad (11)$$

where n is the number of monomers in the aggregate.

Kinetic Data Collection. All kinetic data were obtained at 20 °C and with the exception of slow ANS binding and intermolecular FRET measurements (discussed below) were collected using an Applied Photophysics stopped-flow fluorescence spectrometer equipped with both excitation and emission monochromators (Applied Photophysics, Leatherhead, UK). Excitation slit widths were 4 nm and emission slit widths 6 nm for all measurements. The kinetic traces shown are an average of three or more experiments. Changes in Trp fluorescence upon denaturation were monitored by 10:1 mixing of 4.44 M sequanal grade Gn-HCl with colicin E1 C-terminal thermolytic channel peptide (1 mg/mL) in 100 mM NaCl/10 mM dimethylglutaric acid (DMG) buffer, pH 6.0, to provide a final Gn-HCl concentration of 4 M and a peptide concentration of 0.1 mg/mL.

Tryptophan fluorescence was monitored by 295 nm excitation, and emission was detected at right angles at the characteristic native Trp λ_{em}max of the peptide examined (Merrill *et al*., 1993). For fast ANS binding, the peptide was denatured as described above except that the 4.44 M Gn-HCl solution was made 0.11 mM in ANS concentration to provide a final ANS concentration of 0.1 mM. The sample was excited at 372 nm and emission monitored at 480 nm. Slow ANS binding was monitored as described above with manual mixing using a PTI Alphascan-2 spectrofluorometer (PTI, South Brunswick, NJ) with the excitation slit width at 3 nm and the emission slit width at 6 nm. The time dependence of intermolecular Trp−AEDANS FRET upon denaturation was monitored by manual mixing using the PTI configuration as described above. A solution of equal amounts of Trp^- peptide−AEDANS adduct and WT peptide was mixed as described above to obtain a final Gn-HCl concentration of 4 M and a peptide concentration of 0.1 mg/mL. AEDANS fluorescence intensity (480 nm) was monitored as a function of time upon Trp excitation (295 nm). The "pulse method" as described by Engelhard and Evans (1995) was also used to determine whether ANS had any direct effect on the unfolding of the channel peptide. The results were identical regardless of the method employed for ANS binding.

Data Analysis. Rate constants were calculated by fitting kinetic data by nonlinear least-squares analysis (MicroCal Origin; MicroCal Software Inc., Northhampton, MA). A fit was deemed acceptable if it exhibited random residuals and had reached minimum error in all fitting parameters (standard errors were typically between 5 and 10%). Kinetic traces which showed single exponential kinetics were fit with the equation:

$$F = F_o + F_1[1 - \exp(-kt)]$$

where F is the fluorescence at time t, F_o is the initial fluorescence at time zero, F_1 is the fluorescence change during the unfolding reaction, and k is the rate constant. Kinetic traces which showed double exponential kinetics were fit with the equation:

$$F = F_o + F_1[1 - \exp(-k_1t)] + F_2[1 - \exp(-k_2t)]$$

where F and F_o have the same definitions as above and F_1 and F_2 are the fluorescence changes for the double exponential unfolding reaction with rate constants k_1 and k_2, respectively.

Since peptide dimerization would be second order in peptide concentration, the kinetic trace for the peptide's dimerization was fit using a hyperbolic equation:

$$F = F_o + F_1\{k_{app}t/(1 + k_{app}t)\}$$

The terms F, F_o, t, and F_1 have the same definitions as above, and k_{app} is the apparent rate constant for the dimerization process where $k_{app} = k[P]_o$ and k is the second-order rate constant of dimerization which is dependent on the concentration of the monomeric protein species P.

RESULTS

Size-Exclusion Chromatography. The peptide's denaturation in Gn-HCl was monitored by size-exclusion HPLC (Figure 1). From 0 to 2 M Gn-HCl, the channel peptide eluted as a single peak with a calculated R_S between 21 and 24 Å. At 4 M Gn-HCl, the presence of aggregated protein,

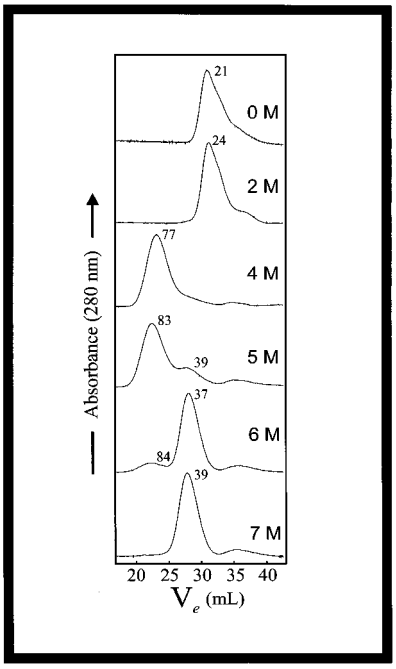

FIGURE 1: Size-exclusion HPLC elution chromatograms of colicin E1 channel peptide in Gn-HCl. The peptide's elution (elution volume, V_e) was detected by the UV absorbance at 280 nm. The column was equilibrated to the appropriate Gn-HCl concentration (M) as indicated in the figure and calibrated with protein standards ($r = 0.997$ for least-squares linear regression analysis) as described under Materials and Methods. The calculated Stokes' radii (Å) are shown for each peak.

likely a mixture of higher order aggregates (dimer, trimer, and tetramer), was evident by a shift to a smaller elution volume corresponding to a Stokes' radius of 77 Å (with the expected peak broadening for a heterogeneous distribution of peptide aggegrate states). With increasing concentration of Gn-HCl, above 5−6 M, a second peak appeared, with a Stokes' radius of about half that of the earlier peak (~40 Å). In 7 M Gn-HCl, only one peak was observed with a 39 Å Stokes' radius, suggesting either complete dissociation of the aggregate into monomers or a large shape change of the associated complex from the species observed in 4 M Gn-HCl.

Chemical Cross-Linking and SDS−PAGE Analysis. In order to examine the nature of the aggregated species detected by chromatography, Gn-HCl-denatured peptide was subjected to SDS−PAGE. Using freshly prepared β-mercaptoethanol sample buffer, great care was taken to ensure sufficient reduction of any intermolecular disulfide bonds which may have formed. Electrophoresis demonstrated the presence of a prominent band (band M, Figure 2A) corresponding to the monomer and a less prevalent band (band D, Figure 2A) corresponding to the dimer species of the channel peptide. It was also noticed that a faint band corresponding to the presence of the trimer species was visible from 4 to 6 M GnHCl.

In a second experiment, the peptide was subjected to various denaturant concentrations in the presence of a water-soluble carbodiimide, EDC, which couples carboxyl groups to primary amines resulting in the formation of amide bonds. Following the cross-linking reaction, the protein samples were analyzed by SDS−PAGE, and the results are shown in Figure 2B. The control lane shows untreated channel peptide (no EDC treatment). The other samples contained

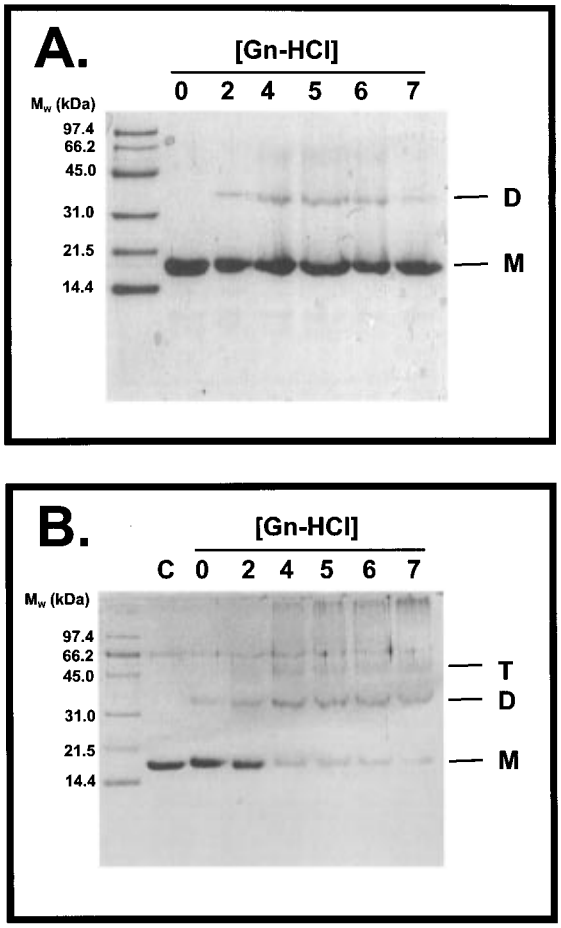

FIGURE 2: (A) Dimerization of Gn-HCl-denatured WT channel peptide detected by SDS−PAGE. The channel peptide was incubated in the denaturant concentrations as indicated in the figure (see unfolding conditions under Materials and Methods) and 10 μg of protein was loaded per gel lane. Band D shows dimerized channel peptide (M_r 36 000) and M monomeric channel peptide (M_r 18 000). Molecular weight standards (top to bottom): phosphorylase B, 97.4 kDa; bovine serum albumin, 66.2 kDa; ovalbumin, 45.0 kDa; carbonic anhydrase, 31.0 kDa; soybean trypsin inhibitor, 21.5 kDa; lysozyme, 14.4 kDa. (B) SDS−PAGE analysis of EDC-cross-linked channel peptide. Channel peptide was incubated with various concentrations of denaturant as indicated, and the conditions for chemical crosslinking were as described under Materials and Methods and 4 μg of protein was loaded per gel lane. T, D, and M correspond to trimer, dimer, and monomer forms of the channel peptide, respectively. The control contains channel peptide with no denaturant or EDC cross-linker reagent. The zero denaturant contains 10 mM EDC but no denaturant. Molecular weight standards were as in (A) above.

EDC that had been allowed to react with the protein for 1 h at 20 °C. The sample containing no denaturant (with EDC) remained predominantly in the monomer form with faint bands corresponding to the dimer and trimer forms. Upon increasing denaturant concentration, the monomer band steadily decreased in intensity while the dimer and trimer bands increased with the dominant band in 4 M Gn-HCl corresponding to the dimer form of the channel peptide. However, at 7 M Gn-HCl, the dimer and trimer band intensities decreased with considerably higher molecular weight aggregates becoming visible near the interface between the stacking and resolving gels.

Intermolecular Fluorescence Resonance Energy Transfer. To confirm peptide aggregation in solution upon denaturation (4 M Gn-HCl), Trp (donor) to AEDANS (acceptor) intermolecular fluorescence resonance energy transfer (FRET)

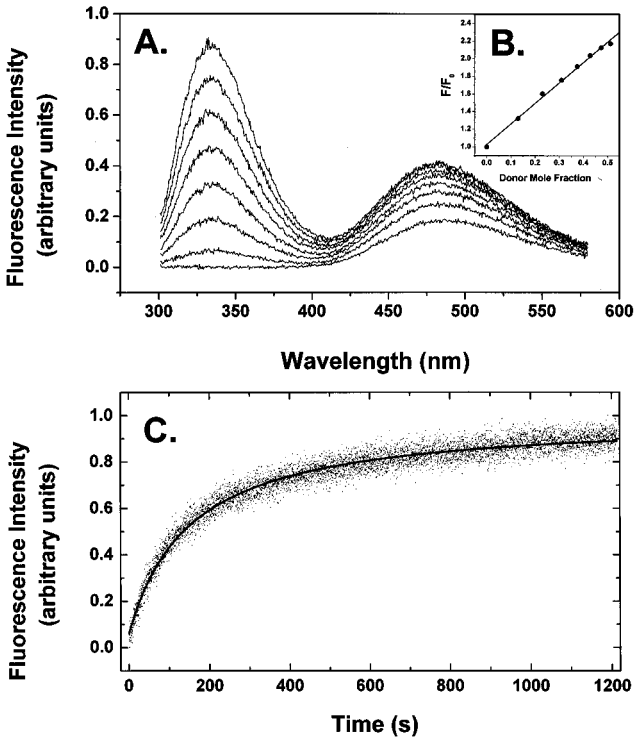

FIGURE 3: (A) Dimerization of Gn-HCl-denatured channel peptide detected by intermolecular Trp−AEDANS FRET. Trp−AEDANS-labeled peptide (0.1 mg/mL) was titrated with WT peptide (excited at 295 nm), and the increase in AEDANS acceptor (λ_{em}max = 480 nm) fluorescence was measured in 4 M Gn-HCl (see Materials and Methods). The increasing intensity in the spectra shown corresponds to the addition of WT channel peptide in 0.015 mg/mL increments (initial and final spectra at 0 and 0.105 mg/mL, respectively). The excitation and the emission band-passes were 3 and 6 nm, respectively. (B) Fluorescence data from *(A)* were fit by least squares linear regression analysis according to the model described under Materials and Methods ($r = 0.998$). (C) Dimerization kinetics of the colicin E1 channel peptide monitored by intermolecular FRET. Data corresponding to the AEDANS fluorescence intensity (480 nm) from the labeled Trp$^-$ peptide upon WT Trp excitation (295 nm) are plotted. Fluorescence data were collected as described under Materials and Methods and were fit with a hyperbolic function (see Materials and Methods) with an apparent rate constant of 0.0066 s^{-1}.

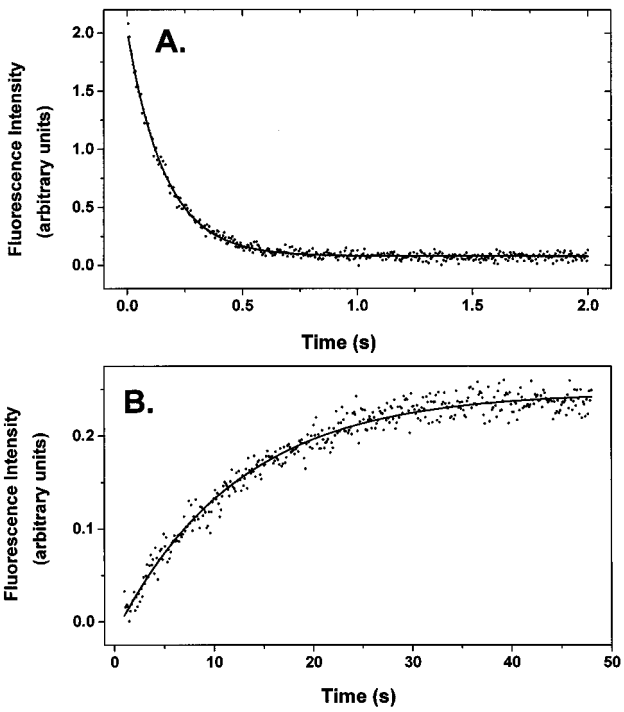

FIGURE 4: Unfolding kinetics of the colicin E1 channel peptide monitored by WT Trp fluorescence. WT Trp fluorescence was monitored at 321 nm with 295 nm excitation. The fast denaturation of the peptide is shown in (A), and the much slower fluorescence rise is shown in (B). Fluorescence data were collected as described under Materials and Methods, and the fast unfolding component was removed from the slow kinetic trace. The data were fit with a single exponential function (see Materials and Methods) with fast (A) and slow (B) rate constants of 2.5 and 0.082 s^{-1}, respectively.

was measured between WT channel peptide (no AEDANS label) and AEDANS-labeled mutant channel peptide devoid of Trp (Trp$^-$). Acceptor fluorescence was measured in the presence of varying amounts of donor species (Figure 3A). Intermolecular Trp−AEDANS FRET was not detected in the native state (0 M Gn-HCl; data not shown). However, intermolecular Trp−AEDANS FRET was observed in 4 M Gn-HCl and was shown to increase upon titration of acceptor (Trp$^-$ peptide−AEDANS adduct) with donor (WT peptide; Figure 3A). Modeling the results using the theoretical model described under Materials and Methods, it was determined that the best fit corresponded to the presence of dimeric peptide (dimer model) at 4 M Gn-HCl (Figure 3B, r = 0.998).

Peptide Association Kinetics. The kinetics for the association of the channel peptide upon denaturation in 4 M Gn-HCl were investigated by observing the time dependence of intermolecular Trp−AEDANS FRET between WT peptide and AEDANS-labeled Trp$^-$ channel peptide. The kinetic trace obtained (Figure 4A) could not be fit by a single exponential equation, or a double exponential equation (see Materials and Methods), as fits using these equations provided nonrandom residuals and abnormally large standard errors in fitting parameters. However, a good fit was obtained when the data were fit with the hyperbolic equation (see Materials and Methods) providing an apparent rate constant of 0.0066 s^{-1} (Table 1). The apparent association rate constant was not, however, dependent on peptide concentration. No change in the apparent dimerization rate constant was observed when the total peptide concentration was varied over a large range (0.005−0.1 mg/mL; data not shown). Furthermore, the rate of the reverse reaction (folding reaction) from 7 M to 4 M Gn-HCl could not be measured since the refolding must be conducted in discrete steps of 0.25 M denaturant.

WT Trp Fluorescence and ANS Binding. WT peptide Trp fluorescence described a fast (fast rate constant, k_f = 6.2 s^{-1}, Table 1) major unfolding transition which fit to a single exponential decay (Figure 4A). A second much slower fluorescence rise (slow rate constant, k_s = 0.082, Table 1) was also observed (Figure 4B). The binding of the fluorescent probe ANS to the peptide upon denaturation was also rapid (k_f = 2.5 s^{-1}, Table 1), and the data fit single exponential kinetics (Figure 5A). However, a subsequent slower increase in ANS binding was also detected (Figure 5B; k_s = 0.012 s^{-1}, Table 1).

Mutant Peptide Trp Fluorescence. The kinetics reported by Trp fluorescence of the individual single Trp mutant peptides were diverse. With the exception of W-367, all of the single Trp mutant peptides reported both a fast unfolding transition followed by a much slower fluorescence change (rate constants k_f and k_s, respectively, Table 1). The kinetic parameters obtained for unfolding of each of the 11 mutant

Table 1: Rate Constants and Half-Lives for the Denaturation and Dimerization of the Colicin E1 Channel Peptide in 4 M Gn-HCl[a]

peptide	k_f (s^{-1})	$t_{1/2(f)}$ (s)	k_s (s^{-1})	$t_{1/2(s)}$ (s)
WT FRET[b]			0.0066 ± 0.0001	110 ± 10
WT ANS[c]	2.5 ± 0.1	0.28 ± 0.01	0.012 ± 0.001	58 ± 5
WT Trp[d]	6.2 ± 0.1	0.11 ± 0.01	0.082 ± 0.002	8.5 ± 0.2
W-355	0.62 ± 0.05	1.1 ± 0.1	0.069 ±0.004	10 ± 0.6
W-367	12 ± 1	0.058 ± 0.005		
W-404	20 ± 2	0.035 ± 0.003	0.30 ± 0.04	2.3 ± 0.3
W-413	11 ± 3	0.063 ± 0.017	0.11 ± 0.02	6.3 ± 1.1
	2.1 ± 0.2	0.33 ± 0.03		
W-424	57 ± 9	0.012 ± 0.001	0.11 ± 0.02	6.3 ± 1.1
	4.0 ± 0.1	0.17 ± 0.01		
W-431	16 ± 3	0.043 ± 0.001	0.12 ± 0.01	5.8 ± 0.5
	4.5 ± 0.7	0.15 ± 0.02		
W-443	0.66 ± 0.03	1.1 ± 0.1	0.026 ± 0.002	27 ± 2
W-460	3.0 ± 0.1	0.23 ± 0.01	0.057 ± 0.003	12 ± 0.6
W-484	18 ± 1	0.039 ± 0.002	0.38 ± 0.01	1.8 ± 0.1
			0.029 ± 0.001	24 ± 1
W-495	14 ± 1	0.050 ± 0.004	0.39 ± 0.10	1.8 ± 0.5
			0.049 ± 0.004	14 ± 1
W-507	5.8 ± 0.2	0.12 ± 0.01	0.0058 ± 0.0005	120 ± 10

[a] Dimerization detected by Trp−AEDANS intermolecular FRET was fit with the hyperbolic function, and all other data were fit with the single or double exponential functions as outlined under Materials and Methods; k_f is the rate constant for the fast major unfolding transition, and k_s is the rate constant for the slower structural rearrangement following the initial denaturation transition. The error shown is the standard error obtained from fitting. Reaction half-lives [$t_{1/2} = \ln(2)/$ rate constant] were calculated from corresponding rate constants. [b] Apparent rate constant determined from Trp−AEDANS intermolecular FRET. [c] Rate constants determined from the binding of the ANS to the peptide upon denaturation. [d] Rate constants determined from WT Trp fluorescence.

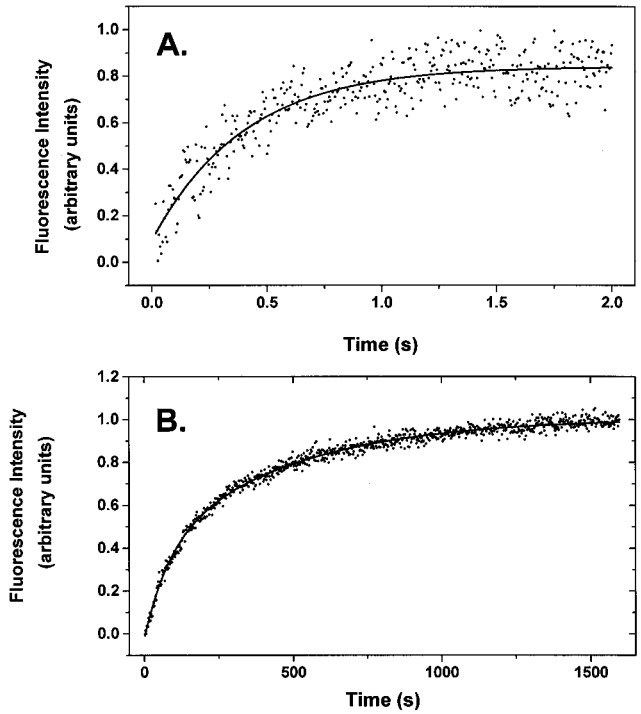

FIGURE 5: Unfolding kinetics of the colicin E1 channel peptide monitored by ANS binding. ANS fluorescence was monitored at 480 nm with 372 nm excitation. ANS binding upon fast denaturation of the peptide is shown in (A), and the slower phase of ANS binding is shown in (B). Fluorescence data were collected as described under Materials and Methods, and the fast unfolding component was removed from the slow kinetic trace. The data were fit with the single exponential function (see Materials and Methods) with fast (A) and slow (B) rate constants of 6.2 and 0.012 s^{-1}, respectively.

peptides are reported in Table 1. However, only a few selected representative kinetic traces are shown for mutant peptides W-355, W-431, W-484, and W-507 (Figure 6A−D). In the fast transition, most single Trp fluorescence kinetic traces fit single exponential kinetics. Interestingly, residues W-413, W-424, and W-431 fit double exponential kinetics, each providing two fast denaturation rate constants (Table 1). A representative kinetic trace for denaturation of single Trp peptide W-431 is shown (Figure 6A, W431-1 and W431-2). Likewise, in the slow unfolding phase the fluorescence kinetics of all single Trp residues but W-484 and W-495 fit single exponential kinetics (Table 1). The large but slow fluorescence rise reported by mutant peptides W-484 and W-495 fit double exponential decay kinetics. A representative kinetic trace for denaturation of single Trp peptide W-484 is shown (Figure 6B, W484-1 and W484-2). Three of the single Trp mutant peptides, W-355, W-443, and W-507, underwent fluorescence increases in the fast phase of the peptide's denaturation in 4 M Gn-HCl. Following the fast unfolding transition, residues W-355 and W-443 each reported a slower fluorescence rise (data shown for W-355, Figure 6C, W355-1 and W355-2). Residue W-507, however, reported a very slow ($k_s = 0.0058$ s^{-1}; Table 1) fluorescence decay following the rapid unfolding transition (Figure 6D, W507-2).

DISCUSSION

Although Gn-HCl is expected to increase protein solubility, it was determined through size-exclusion HPLC, SDS−PAGE, and intermolecular FRET that the intermediate structure which exists in 4 M Gn-HCl consists of a distribution with the major component consisting of two tightly associated, but partially unfolded peptides. Size-exclusion HPLC demonstrated that the structure which persists in 4 M Gn-HCl has an elution volume of 23 mL corresponding to a Stokes' radius of about 80 Å (Figure 1). However, a random coil of ca. 180 amino acid residues would be expected to possess a radius of gyration of about 40 Å and for a dimeric species near 56 Å (Creighton, 1993). Thus, the 178 residue channel peptide, only partially denatured in 4 M Gn-HCl, would be expected to have a Stokes' radius of near 56 Å as opposed to the observed radius of 77 Å. This can likely be explained on the basis of the presence of some higher aggregate species (trimer, tetramer, etc.) which gives rise to the broader than expected peaks. Furthermore, the accuracy of Stoke radii determinations is based on identical solvent systems (viscosity, ion strength, etc.) and does not account for shape changes within the protein (polymer) being sieved. These factors may clearly be interacting and are not controlled for the HPLC analysis of peptide association in these experiments. Indeed, the experimental Stokes' radius of the denatured peptide in 7 M Gn-HCl is 39 Å (Figure 1). Furthermore, the chemical cross-linking results indicate that the peptide is not monomeric at high denaturant but is largely aggregated. The most probable explanation of the combined observations is that there must be a shape change of the aggregate from 5 to 7 M Gn-HCl.

The presence of the dimerized species was confirmed by SDS−PAGE (Figure 2). Although much of the dimer dissociated upon dilution of the samples prior to gel loading (see Materials and Methods), a small amount of dimerized species was detected with the dimer most prevalent at

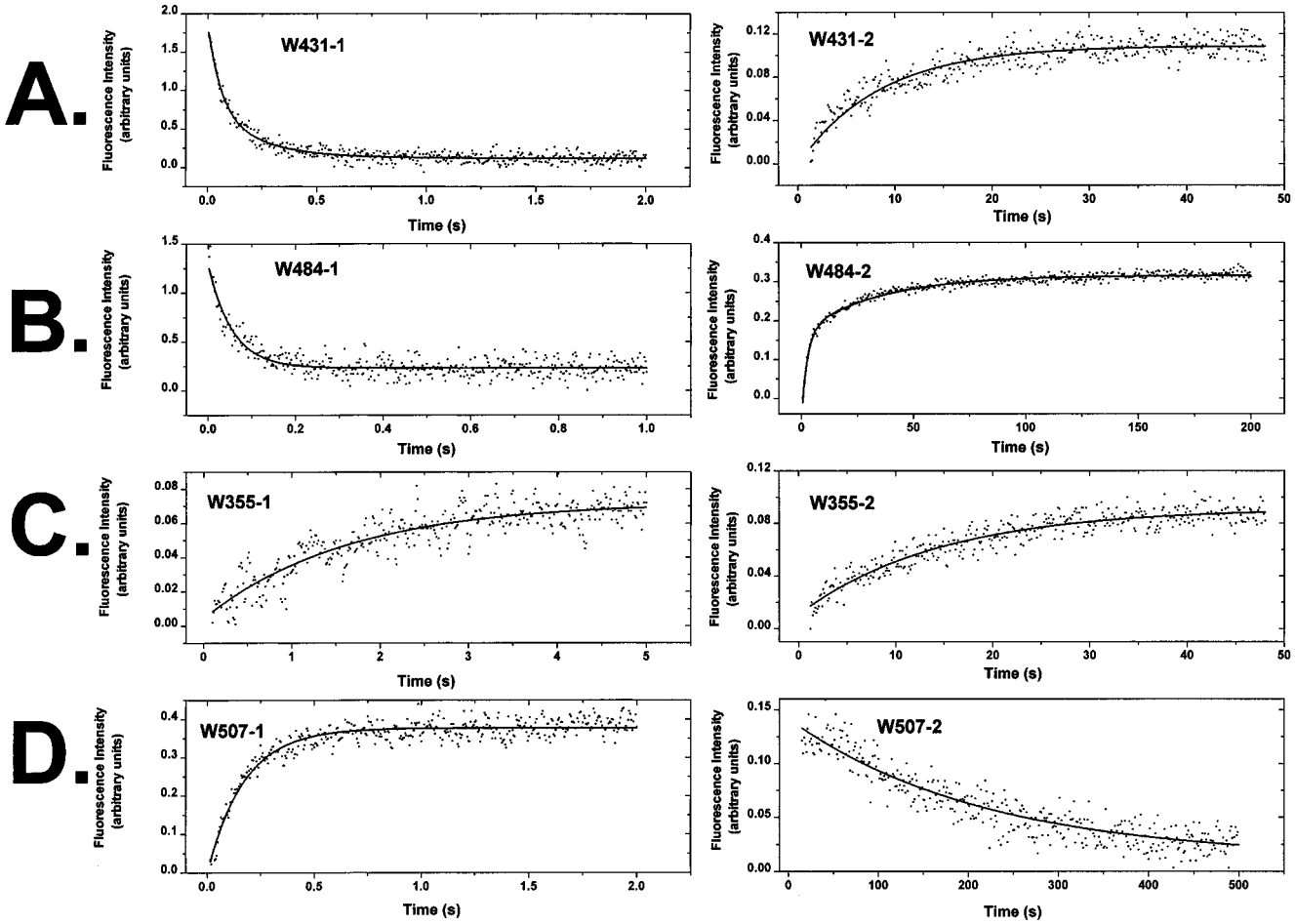

FIGURE 6: Unfolding kinetics of the colicin E1 channel peptides monitored by Trp fluorescence. (A) Unfolding kinetics of W-431 by Trp fluorescence. W-431 Trp fluorescence was monitored at 330 nm with 295 nm excitation. Trace 431-1 shows the fast denaturation of the peptide, and trace 431-2 shows the slower fluorescence rise. Fluorescence data were collected as described under Materials and Methods, and the fast unfolding component was removed from the slow kinetic trace. The fast unfolding trace (W431-1) was fit with the double exponential function with rate constants 16 and 4.5 s^{-1}, and the slow unfolding component (W431-2) was fit with the single exponential function (see Materials and Methods) with a rate constant of 0.12 s^{-1}. (B) Unfolding kinetics of W-484 by Trp fluorescence. W-484 Trp fluorescence was monitored at 322 nm with 295 nm excitation. Trace 484-1 shows fast denaturation of the peptide, and trace 484-2 shows the slower fluorescence rise. Fluorescence data were collected as described under Materials and Methods, and the fast unfolding component was removed from the slow kinetic trace. The fast unfolding trace (W484-1) was fit with the single exponential function with a rate constant of 18 s^{-1}, and the slower unfolding component (W484−2) was fit with the double exponential function (see Materials and Methods) with rate constants 0.38 and 0.029 s^{-1}. (C) Unfolding kinetics of W-355 by Trp fluorescence. W-355 Trp fluorescence was monitored at 329 nm with 295 nm excitation. Trace W355-1 shows the fast denaturation of the peptide, and trace W355-2 shows the slower fluorescence rise. Fluorescence data were collected as described under Materials and Methods, and the fast unfolding component was removed from the slow kinetic trace. The data were fit with the single exponential function (see Materials and Methods) with fast (W355-1) and slow (W355-2) rate constants of 0.62 and 0.069 s^{-1}, respectively. (D) Unfolding kinetics of W-507 by Trp fluorescence. W-507 Trp fluorescence was monitored at 322 nm with 295 nm excitation. Trace W507-1 shows the fast denaturation of the peptide, and trace W507-2 shows the slower fluorescence decay characteristic of W-507. Fluorescence data were collected as described under Materials and Methods, and the fast unfolding component was removed from the slow kinetic trace. The data were fit with the single exponential function (see Materials and Methods) with fast (W507-1) and slow (W507-2) rate constants of 5.8 and 0.0058 s^{-1}, respectively.

intermediate Gn-HCl concentrations around 4 M. The channel peptide contains a single buried cysteine residue (amino acid position 505), and it is plausible that dimerization results from the formation of an intermolecular disulfide bond between two unfolded monomeric peptides. However, the dimerized peptide was detected by SDS−PAGE in the presence of β-mercaptoethanol or dithiothreitol despite numerous experiments and controls to ensure that no disulfide bonds were present. SDS−PAGE analysis following chemical cross-linking with EDC provided the definitive answer to the aggregate state of the channel peptide. The predominant species present at intermediate denaturant concentration is the dimer but other aggregate states are also present, although in lower amounts. To complement HPLC and SDS−PAGE data, dimerization was detected in solution by FRET measurements. Intermolecular Trp−AEDANS FRET (Figure 3A) was observed in 4 M Gn-HCl and was shown to increase upon titration of acceptor with donor, demonstrating the presence of heterodimers consisting of WT peptide and AEDANS-labeled Trp^- mutant peptide. The fluorescence data data fit the dimeric model and clearly did not fit trimeric, tetrameric, or higher aggregate models (data not shown).

The apparent rate constant of dimer formation was measured by monitoring the time dependence of Trp−AEDANS intermolecular FRET between WT peptide and AEDANS-labeled Trp^- peptide (Figure 3C). Dimerization kinetic data could not be fit with an exponential but were readily fit by the hyperbolic equation. The apparent dimerization rate constant (k_{app} = 0.0066 s^{-1}, $t_{1/2}$ = 105 s),

however, could not be shown to be dependent on overall peptide concentration within the limits of detection (0.005−0.1 mg/mL, data not shown). Since peptide dimerization is believed to involve hydrophobic association between the nonpolar cores of partially unfolded peptide monomers, the process of peptide dimerization would likely occur after significant peptide unfolding. Thus, the apparent dimerization rate constant would be dependent on the concentration of a partially unfolded intermediate structure which is a prerequisite for dimerization rather than on the initial native peptide concentration. In this mechanism, the appearance of this partially unfolded intermediate species, first order in peptide concentration, would be the rate-limiting step of denaturation which gives rise to the apparent slow formation of the dimer ($k_{app} = 0.0066$ s^{-1}).

Although peptide unfolding detected by WT Trp fluorescence was fast ($k_f = 6.2$ s^{-1}, $t_{1/2} = 112$ ms) and the fluorescence change was large (Figure 4A), indicating a significant degree of unfolding in the millisecond time range, a much slower Trp fluorescence increase, fit to single exponential kinetics ($k_s = 0.082$ s^{-1}, $t_{1/2} = 8.5$ s), was also observed. Similarly, although the binding of ANS to the peptide upon denaturation (Figure 5A) detected the exposure of nonpolar surface area (fluorescence increase) in the millisecond time range ($k_f = 2.5$ s^{-1}, $t_{1/2} = 277$ ms) concomitant with peptide denaturation detected by WT Trp fluorescence, a second slow phase of ANS binding, fit to a single exponential, was also detected (Figure 5B; $k_s = 0.012$ s^{-1}, $t_{1/2} = 58$ s). These data are suggestive of a "structural re-coil" effect where the peptide's core residues reassemble somewhat following a rapid and large initial unfolding transition. The channel peptide is unusually hydrophobic, and the region of the peptide which retains structure in the dimerized intermediate contains only hydrophobic residues (Steer & Merrill, 1995). It is likely that dimerization of the channel peptide upon Gn-HCl -induced unfolding results from strong hydrophobic interaction between partially denatured monomers. Assembly and packing of the peptide's core residues, following initial denaturation, may result in the formation of a structural prerequisite to dimerization consisting of a nonpolar scaffold of hydrophobic residues.

The local unfolding rate constants provided by the various single Trp mutant peptides are shown in Table 1. It should be noted that although changes in the Trp fluorescence of the single Trp mutant peptides upon denaturation will provide local kinetic unfolding information it is possible that local structural perturbations, attributed to aromatic substitutions within these mutant peptides, do have an effect on the local unfolding rate constants of the single Trp mutant peptides. Although it was shown that the introduction of single Trp residue peptides does not significantly alter the peptide's native structure or unfolding equilibria (Steer & Merrill, 1995), the rate of the peptide's unfolding may be sensitive to the Trp substitutions. The evidence for the suitability of the single Trp mutant peptides for study can be summarized as follows: (1) All of the single Trp mutants have both *in vivo* and *in vitro* channel-forming activity similar to the WT peptide (Steer & Merrill, 1995). (2) Protein secondary structure of the mutant peptides was analogous to that of the WT peptide (ca. 47% α-helix) as determined by CD spectroscopy. (3) The unfolding profiles of the mutant peptides were analogous to the WT unfolding profiles as monitored by ANS binding. (4) Expression levels of the mutant proteins were all comparable to the WT, and purification appeared to proceed normally in all cases.

Single Trp residues W-355, W-443, and W-507 underwent increases in fluorescence intensity upon denaturation (Figure 6C,D, W355-1 and W507-1; W-443 data not shown). It is a possibility that these fluorescence increases result from peptide dimerization, which might shield these residues from solvent, thus increasing their fluorescence intensity. However, the larger rate constants of unfolding reported by residues W-355, W-443, and W-507 (0.62, 0.66, and 5.8 s^{-1}, respectively) suggest that these fluorescence changes precede dimerization. The increase in the fluorescence intensity of residue W-507 most likely results from the alleviation of intrinsic quenching by the nearby cysteine residue at position 505. It has also been suggested previously that the fluorescence of residues W-355 and W-443 is intrinsically quenched in the native peptide (Steer & Merrill, 1995). Similar fluorescence intensity changes of single Trp mutant peptides upon protein denaturation have been observed elsewhere (Beechem *et al.*, 1995).

The N-terminal residues W-367 and W-404 are located in peptide segments which unfold relatively early in the unfolding process (Steer & Merrill, 1994; rate constants 12 and 20 s^{-1}, respectively; Table 1, kinetic traces not shown). Interestingly, the unfolding rate constant reported by W-355, also located in this N-terminal segment, is much slower at 0.62 s^{-1}. It was recently suggested that helix 1 of the thermolytic colicin E1 channel peptide is not really part of the peptide but rather it constitutes a portion of a long helix which links the colicin E1 channel-forming domain to the receptor binding domain (Stauffacher, 1996). This idea is supported by the recently solved crystal structure of the pore-forming colicin Ia, a close relative of colicin E1 (Weiner *et al.*, 1996). The colicin Ia structure revealed that the first helix of its channel-forming domain is actually a long helix linker which connects the channel domain to the receptor binding domain. Thus, if helix 1 of the colicin E1 channel peptide is actually a linker, rather than a helix associated with the peptide, it might not unfold concomitantly with the N-terminal peptide segment housing residues W-367 and W-404.

Peptide unfolding detected by Trp residues W-413, W-424, and W-431 was also fast but did not fit single exponential kinetics. The data could only be fit by a double exponential equation (see Materials and Methods) which assigned two fast unfolding rate constants to the kinetic denaturation traces (Table 1). A representative trace is shown for W-431 mutant peptide denaturation (Figure 6A, W431-1; W-413 and W-424 traces not shown). Clearly the structural rearrangements occurring in this region upon peptide denaturation are complex. A significant portion of this region of the peptide is nonhelical and forms a large extended loop in the native structure. Certainly, upon denaturation, this loop would be expected to behave differently than the more structurally ordered helical segments of the peptide. Although Gn-HCl-induced unfolding does not activate the peptide, it is interesting that these three residues are located in the peptide's gating segment which has been shown to be involved in a significant structural rearrangement upon low pH-induced activation (Steer *et al.*, 1996).

Residues in the peptide's C-terminal region fit single exponential unfolding kinetics and reported fast unfolding with rate constants ranging from 3.0 s^{-1} (W-460) to 18 s^{-1}

(W-484). The unfolding rate constants of the peptide segment containing residues W-484 and W-495 (18 and 14 s^{-1}, respectively) were similar to the rate constants reported by residues W-367 and W-404 (12 and 20 s^{-1}, respectively). Residues W-484 and W-495 are located in a buried and hydrophobic region of the peptide beneath the peptide's N-terminal helices 1 and 2 (Elkins *et al.*, 1995). Unfolding of the peptide's N-terminal segment would likely expose the core residues W-484 and W-495. Thus, it is probable that the unfolding rate constants observed for Trp residues W-484 and W-495 primarily reflect the rapid denaturation of the peptide's N-terminal locale in 4 M Gn-HCl.

With the exception of W-367, each single Trp residue detected a slower structural rearrangement (Figure 6A−D, W431-2, W484-2, W355-2, and W507-2; Table 1) following the more rapid initial unfolding event with rate constants ranging from 0.0058 s^{-1} (W-507) to 0.39 s^{-1} (W-495). These slower fluorescence changes occur after the peptide's major unfolding transition, and all of the single Trp residues involved in the slower phase reported a fluorescence increase with the exception of W-507, which reported a fluorescence decrease. As discussed above for the WT peptide, these fluorescence changes most likely represent a slow rate-limiting step which precedes dimerization. The largest and most significant fluorescence increases were provided by core Trp residues W-484 and W-495, and the traces fit double exponential kinetics (Figure 6B, W484-2, trace shown for W-484 only). The large increase in fluorescence reported by these residues is consistent with the finding that the intermediate structure primarily encompasses the peptides C-terminal hydrophobic core (Steer & Merrill, 1995).

The slow fluorescence decrease reported by residue W-507 is interesting. As discussed earlier, the association and packing of hydrophobic residues likely occur during dimerization. Therefore, during the unfolding process, dimerization could result in alleviation of some internal quenching of W-507 caused by the adjacent residue C-505. It is also possible that the peptide segment in the region of W-507 unfolds very slowly and that the fluorescence decrease is the result of further exposure of W-507 to solvent following the initial major unfolding transition. Indeed it was previously shown by fluorescence quenching experiments that W-507 is the most buried of all 11 single Trp residues (Merrill *et al.*, 1993).

This kinetic study has shown that single Trp residues in the colicin E1 channel peptide do experience specific unfolding events with individually characteristic kinetics. The results are consistent with a fast initial major denaturation phase followed by a slower phase of hydrophobic core residue assembly followed by dimerization. Combining the results of this study and the results of Steer and Merrill (1995), a model to describe the kinetic unfolding mechanism of the channel peptide upon treatment with 4 M Gn-HCl is proposed (Figure 7). The bulk of the peptide is denatured in the rapid unfolding transition (fast unfolding rate constant k_f). The resultant structure possesses little native structure, but its hydrophobic core is partially intact. Due to the hydrophobic interaction, amplified by the ionic nature of Gn-HCl, the exposed nonpolar core residues slowly assemble (slow rate constant k_s), forming a structural prerequisite to dimerization consisting of a large cluster of hydrophobic residues. Dimerization occurs quickly (with an immeasurable rate constant k_D); hence, the rate-limiting step of hydrophobic assembly with rate constant k_s is observed. It should be noted that refolding of the 4 M Gn-HCl denatured channel peptide necessitates stepwise dilution and requires several hours to complete (Steer & Merrill, 1995). This slow and stepwise refolding indicates that at least one of the reverse rate constants (k_{-f}, k_{-s}, or k_{-D}) is quite small and makes difficult the calculation of the folding/unfolding equilibrium constant from the folding/unfolding rate constants. Further experiments including the analysis of the effects of ionic strength, temperature, and denaturant concentration on the kinetics of the peptide's unfolding may help provide a better understanding of the significance of these site-specific unfolding data.

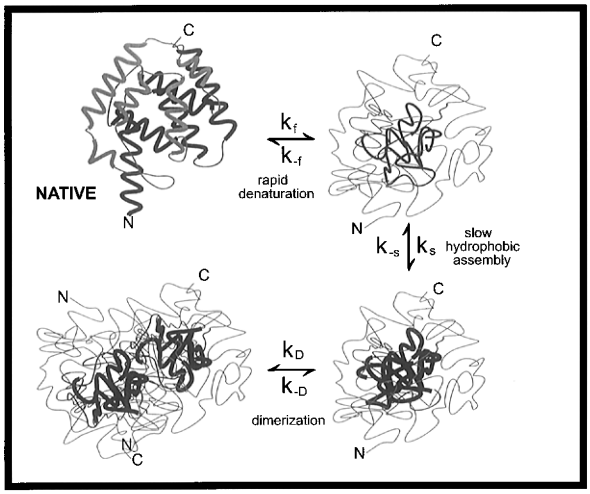

FIGURE 7: Proposed model to illustrate the kinetic unfolding and dimerization mechanism of the colicin E1 channel peptide upon denaturation in 4 M Gn-HCl. The model is based on the preliminary crystal structure of the channel peptide (Elkins *et al.*, 1995), and only the general topology of the helices is implied. The native peptide is unfolded rapidly (rate constant k_f) to a partially denatured structure. The peptide's core residues then assemble slowly by hydrophobic association (rate constant k_s) forming structures prerequisite to dimerization. Dimerization occurs quickly (rate constant k_D) following the rate-limiting step of hydrophobic assembly.

ACKNOWLEDGMENT

We thank Dr. Irwin Tessman for supplying the *E. coli* strain IT3661. We also thank Joseph Briante for purifying the colicin E1 channel peptide and Ariel DiNardo for assistance with HPLC experiments.

REFERENCES

Beattie, B. K., & Merrill, A. R. (1996) *Biochemistry 35*, 9042−9051.

Beechem, J. M., Sherman, M. A., & Mas, M. T. (1995) *Biochemistry 34*, 13943−13948.

Buisson, M., & Reboud, A. M. (1982) *FEBS Lett. 148*, 247−250.

Bullock, J. O. (1992) *J. Membr. Biol. 125*, 255−271.

Bullock, J. O., Cohen, F. S., Dankert, J. R., & Cramer, W. A. (1983) *J. Biol. Chem. 258*, 9908−9912.

Cleveland, M. B., Slatin, S., Finkelstein, A., & Levinthal, C. (1983) *Proc. Natl. Acad. Sci. U.S.A. 80*, 8706−8710.

Cramer, W. A., Dankert, J. R., & Uratani, Y. (1983) *Biochim. Biophys. Acta 737*, 173−193.

Cramer, W. A., Cohen, F. S., Merrill, A. R., & Song, H. Y. (1990) *Mol. Microbiol. 4*, 519−526.

Cramer, W. A., Heymann, J. B., Schendel, S. L., Deriy, B. N., Cohen, F. S., Elkins, P. A., & Stauffacher, C. V. (1995) *Annu. Rev. Biomol. Struct. 24*, 611−641.

Elkins, P. A., Bunker, A., Cramer, W. A., & Stauffacher, C. V. (1995) *Biophys J 68*, A369.

Engelhard, M., & Evans, P. A. (1995) *Protein Sci. 4*, 1553−1562.

Gould, J. M., & Cramer, W. A. (1977) *J. Biol. Chem. 252*, 5491−5497.

Laemmli, U. K. (1970) *Nature (London) 227*, 680−685.

Merrill, A. R., Palmer, L. R., & Szabo, A. G. (1993) *Biochemistry 32*, 6974−6981.

Peterson, A. A., & Cramer, W. A. (1987) *J. Membr. Biol. 99*, 197−204.

Schendel, S. L., & Cramer, W. A. (1994) *Protein Sci. 3*, 2272−2279.

Stauffacher, C. V. (1996) *Biophys. J. 70*, A121.

Steer, B. A., & Merrill (1994) *Biochemistry 33*, 1108−1115.

Steer, B. A., & Merrill (1995) *Biochemistry 34*, 7225−7233.

Steer, B. A., & Merrill (1996) *Biophys. J. 70*, W360A.

Steer, B. A., Szabo, A. G., & Merrill, A. R. (1996) *Biophys. J. 70*, M5A.

Weiner, M. C., Freymann, D. M., Ghosh, P., Finer-Moore, J., & Stroud, R. M. (1996) *Biophys. J. 70*, A140.

BI961926F